Available online at www.sciencedirect.com
ScienceDirect
Ceramics International 35 (2009) 3217–3220
CERAMICS INTERNATIONAL
www.elsevier.com/locate/ceramint

Densification rate and phase structure changes during sintering of zinc titanate ceramics

M.V. Nikolic [a,*], N. Labus [b], M.M. Ristic [b]

[a] Institute for Multidisciplinary Research, Kneza Viseslava 1, 11000 Beograd, Serbia
[b] Institute of Technical Sciences of SASA, Knez Mihailova 35, 11000 Beograd, Serbia

Received 13 January 2009; received in revised form 10 April 2009; accepted 17 May 2009
Available online 18 June 2009

Abstract

Densification rate and phase structure changes during sintering of nanosized $ZnTiO_3$ were studied. Sintering was performed in a dilatometer in two regimes: the first to 900 °C (heating rates 5, 10 and 15 °C/min) and the second to 1200 °C (heating rates 3, 5 and 10 °C/min). XRD analysis of samples sintered at both temperatures combined with Rietveld structure refinement enabled determination of all phases present and their structure parameters. Samples sintered to 900 °C contained $ZnTiO_3$ and Zn_2TiO_4 with traces of r-TiO_2 (rutile) and $Zn_2Ti_3O_8$, while samples sintered to1200 °C contained only r-TiO_2 and Zn_2TiO_4. A master sintering curve was defined for sintering to 900 °C enabling determination of the sintering process activation energy as 313 kJ/mol.
© 2009 Elsevier Ltd and Techna Group S.r.l. All rights reserved.

Keywords: A. Sintering; B. X-ray methods; B. Microstructure; Zinc titanate

1. Introduction

Zinc titanates are promising candidates for low-temperature sintering dielectrics [1,2]. Much work has been devoted to the synthesis of $ZnTiO_3$ powder [3,4]. Dopants have been added to reduce the sintering temperature, but practical applications are partly restricted due to unstable dielectric properties originating from complex phase transitions [5].

Three compounds exist in the ZnO–TiO_2 system. Zn_2TiO_4 (zinc orthotitanate) has an inverse cubic spinel structure ($Fd\bar{3}m$) and is stable from room temperature to its melting (liquid) temperature. $ZnTiO_3$ (zinc metatitanate) has a hexagonal ilmenite structure ($R\bar{3}$), a variant of the corundum structure where the cations are ordered into two non-equivalent oxygen sites. Zinc metatitanate is stable from room temperature to about 945 °C. $Zn_2Ti_3O_8$ was first determined by Yamaguchi et al. [6] as a low temperature form of $ZnTiO_3$ having a defect cubic spinel structure with ordered cation vacancies leading to degradation of the space group symmetry from $Fd\bar{3}m$ to $P4_332$ [7,8]. Taking into account the binary phase diagram for ZnO–TiO_2 [9] and literature data [3–7] the phase transitions in this system, for the ZnO:TiO_2 = 1:1 powder ratio are:

$$\begin{aligned} &ZnO + TiO_2 \overset{\approx 700^\circ C}{\longrightarrow} ZnTiO_3 \overset{700-820^\circ C}{\longrightarrow} \\ &ZnTiO_3 + Zn_2TiO_4 + Zn_2Ti_3O_8 \overset{820-900^\circ C}{\longrightarrow} \\ &ZnTiO_3 + Zn_2TiO_4 + Zn_2Ti_3O_8 + TiO_2 \overset{\geq 950^\circ C}{\longrightarrow} Zn_2TiO_4 + TiO_2 \end{aligned} \quad (1)$$

Sintering is a very complex process and it usually involves several diffusion mass transport mechanisms. It is accompanied by changes in the microstructure [10,11]. If one diffusion mechanism is dominant then, according to Su and Johnson [12], the densification rate can be defined as:

$$\frac{1}{\rho}\frac{d\rho}{dt} = 3\frac{\Omega\gamma D_0}{k_B}\frac{\Gamma(\rho)}{G^n}\frac{e^{-Q/RT}}{T} = AF(\rho)\theta(T) \quad (2)$$

where ρ is the relative density, t is time, Ω is the atomic volume, γ is the surface energy, D_0 is the diffusion coefficient, G is the mean grain size, Q is the apparent activation energy, R is the gas constant, T is the absolute temperature and $\Gamma(\rho)$ is a scaling factor describing features in the microstructure characterizing the microstructural geometry. When the terms related to microstructural and materials properties and terms related to the

* Corresponding author. Tel.: +381 112637367; fax: +381 113055289.
E-mail addresses: mariav@rcub.bg.ac.rs, mariavesna@cms.bg.ac.yu (M.V. Nikolic).

0272-8842/$36.00 © 2009 Elsevier Ltd and Techna Group S.r.l. All rights reserved.
doi:10.1016/j.ceramint.2009.05.028

heating schedule are separated, then A includes all constants, $F(\rho) = \Gamma(\rho)/G^n$ and is a function only of density and $\theta(T)$ is a function only of temperature. The conventional master sintering curve (MSC) defined by Su and Johnson [12] links the work-of -sintering, θ and the density at time t during the thermal cycle, starting at $t = 0$. It is unique for a given powder and green body process and is independent of the sintering path. More recently, the MSC was redefined to be a sigmoidal (S-shape) curve [11,13]:

$$\rho = \rho_0 + \frac{1-\rho_0}{1+\exp(-(\ln\theta + a/b))} \quad (3)$$

where ρ_0 is the relative density at the start of sintering, a and b are constants defining the curve enabling a better fit between the relative sintering density and $\ln\theta$.

The purpose of this work was: (a) a detailed study of sintering of nanosized $ZnTiO_3$ powder to 900 °C through changes in the densification rate enabling determination of a master sintering curve and the sintering process activation energy and (b) sintering to 1200 °C enabling analysis of the phase transformation of $ZnTiO_3$ to Zn_2TiO_4 and r-TiO_2 through changes in the sample densification rate, phase structure and microstructure.

2. Experimental

Starting $ZnTiO_3$ powder (Aldrich, purity 99.5%, particle size < 80 nm) was pressed on a Hydraulic press RING P-14, VEB THURINGER under 98 MPa into pellets 8 mm in diameter and then sintered in a Bähr Gerätebau Type 802s dillatometer with a tube furnace. The green samples were sintered in the following way: first series to 900 °C with three heating rates (5, 10 and 15°/min), hold time 68 min and cooling to room temperature with a cooling rate of 10°/min and second series to 1200 °C with three heating rates (3, 5 and 10°/min), hold time 60 min and cooling to room temperature with a cooling rate of 10°/min.

X-ray analysis was performed on a Seifert MZ IV diffractometer with a Seifert ID 3000 high voltage generator, step 0.02°, hold time 10 s. Structural refinement was carried out by the Rietveld method using the GSAS package [14] with the EXPGUI graphical user interface [15]. Samples were analyzed for the presence of $ZnTiO_3$, Zn_2TiO_4, $Zn_2Ti_3O_8$ and r-TiO_2 (rutile). $ZnTiO_3$ was refined as hexagonal, space group $R\bar{3}$ (rhombohedral cell), $a = 5.07833(3)$, $c = 13.927(1)$ Å, $Z = 6$ [16]. Starting values for atom parameters of $ZnTiO_3$ were taken from the refinement of $FeTiO_3$ performed by Wechsler and Prewitt [17]. All parameters were varied. Starting values for cubic Zn_2TiO_4 (space group $Fd\bar{3}m$) were taken from Millard et al. [18]. The cation distribution was assumed to be completely inverse and only the cell parameters were varied. Starting values for $Zn_2Ti_3O_8$ assuming a defect cubic spinel structure (space group $P4_332$) were taken from Steinike and Wallis [8]. Starting values for r-TiO_2 (rutile–space group $P4_2/mnm$) were taken from Meagher and Lager [19].

3. Results and discussion

The determined average green sample density was 2.34 g/cm^3 (45.3% of the theoretical density of $ZnTiO_3$ of 5.16 g/cm^3 [16]). Obviously denser green samples could be obtained by applying higher pressures, but as the particle size of the starting powder was small it was difficult to obtain green samples that did not laminate prior to sintering when higher pressures were applied.

XRD analysis of samples sintered to 900 °C, show that they consist of mainly $ZnTiO_3$ with some Zn_2TiO_4 and r-TiO_2 and traces of $Zn_2Ti_3O_8$ (Fig. 1). Besides peaks noted for $ZnTiO_3$ we can note the most prominent peaks for Zn_2TiO_4– (2 2 0) and (3 1 1) and the most prominent peak (1 1 0) for r-TiO_2. The determined phase composition and cell parameters ($R_{wp} = 0.0525$) were 81.096 wt.% $ZnTiO_3$ $a = 5.07315$, $c = 13.91768$ (density 5.180 g/cm^3), 14.343 wt.% Zn_2TiO_4 $a = 8.44931$ (5.344 g/cm^3), 2.805 wt.% r-TiO_2 $a = 4.58533$, $c = 2.95652$ (4.269 g/cm^3) and 1.756 wt.% $Zn_2Ti_3O_8$ $a = 8.40648$ (4.500 g/cm^3). The structural parameters obtained for $ZnTiO_3$ are given in Table 1. Bond valence states in $ZnTiO_3$ were calculated from the determined bond lengths using VaList [20] and they were Zn = 1.893; Ti = 4.252 and O = 2.048. The value of the lattice parameter determined for Zn_2TiO_4 is slightly lower than the literature value of Millard et al of $a = 8.46948$ [18]. The decrease in the lattice parameter value

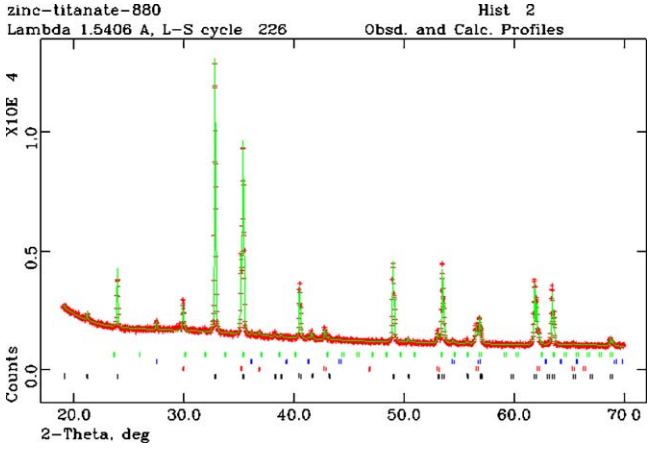

Fig. 1. Rietveld plot (program GSAS) with observed and calculated XRD patterns for the samples sintered to 900 °C (the peak positions of different phases are shown as small solid bar markers at the bottom of the figure in the following order from top to bottom: $Zn_2Ti_3O_8$, r-TiO_2, Zn_2TiO_4 and $ZnTiO_3$).

Table 1
Structural parameters obtained for $ZnTiO_3$.

Atom	x	y	z	U_{iso}
Zn	0	0	0.360643	0.00720
Ti	0	0	0.145423	0.00809
O	0.326469	0.025956	0.244553	0.00813

Metal-oxygen bond lengths (Å)			
Zn-O	2.26998(3)	Ti-O	2.10851(2)
Zn-O	2.02952(2)	Ti-O	1.82770(2)

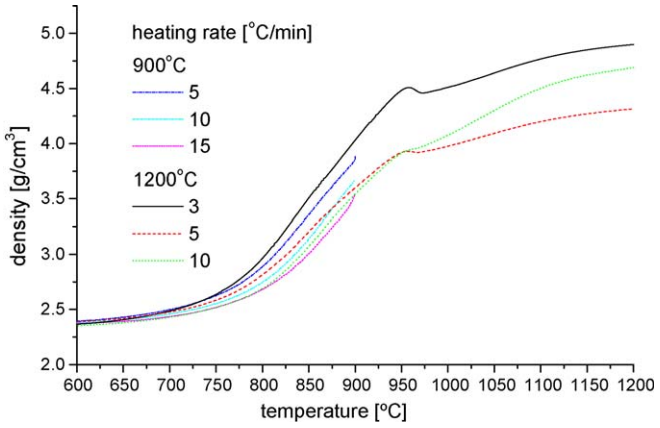

Fig. 2. Density as a function of temperature for samples sintered to 900 and 1200 °C.

indicates that some excess titanium has been incorporated into the Zn_2TiO_4 crystal lattice [7]. Rutile solubility in zinc orthotitanate is up to 0.33 mole at temperatures below 945 °C. At temperatures above 820 °C $Zn_2Ti_3O_8$ if present decomposes to Zn_2TiO_4 and r-TiO_2 where rutile is incorporated into the cubic spinel lattice of zinc orthotitanate until saturation is reached after which a composite phase of rutile and zinc orthotitanate can be observed. Also, at 900 °C $ZnTiO_3$ starts to decompose into Zn_2TiO_4 and rutile [15]. This is the reason why in samples after sintering at 900 °C besides $ZnTiO_3$ we observed Zn_2TiO_4 and r-TiO_2 with only traces of $Zn_2Ti_3O_8$.

Using shrinkage data obtained from dilatometric experiments the sample density was determined as:

$$\rho(t) = \frac{\rho_0}{(1 - (\Delta L(t)/L_0))^3} \quad (4)$$

where ρ_0 is the starting sample density, L_0 is the initial sample length and $\Delta L(t)$ is the change of sample length and t is time. Fig. 2 shows the dependence of the density on temperature for samples sintered to 900 °C using different heating rates. The final sample density is on average 87.2%. A master sintering curve was determined using this density data in the temperature range 600–900 °C and the MSC software [11] and it is shown in Fig. 3. The activation energy was determined through minimizing the error between the experimental data and the MSC

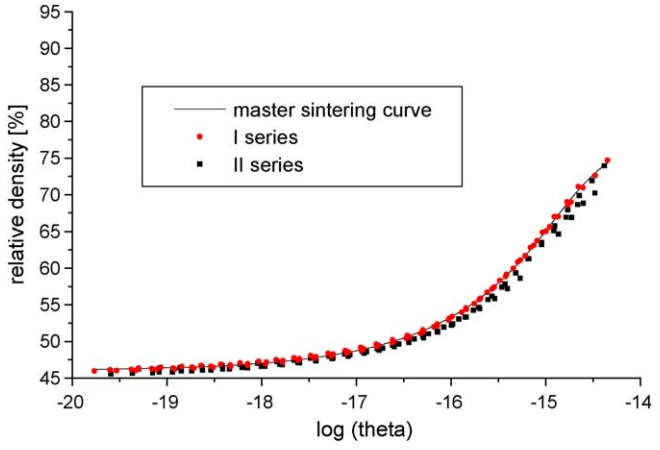

Fig. 3. Master sintering curve in the temperature range 600–900 °C.

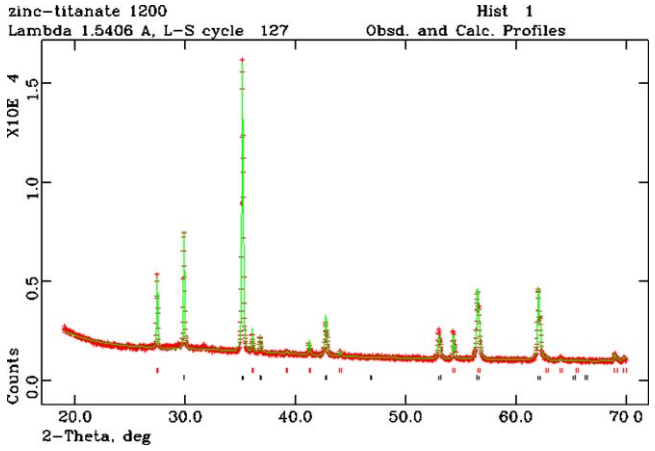

Fig. 4. Rietveld plot (program GSAS) with observed and calculated XRD patterns for the samples sintered to 1200 °C (the peak positions of different phases are shown as small solid bar markers first r-TiO_2 and then Zn_2TiO_4).

model as 313 kJ/mol. Thus, in this temperature range one sintering mechanism is dominant.

XRD analysis of samples sintered to 1200 °C shows that at this temperature Zn_2TiO_4 and r-TiO_2 are present (Fig. 4). The determined phase composition and cell parameters are: 75.93 wt.% Zn_2TiO_4 (density 5.331 g/cm^3) $a = 8.455931$, $u = 0.262041$, degree of inversion assumed to be $x = 1$ and 24.07 wt.% r-TiO_2 (4.248 g/cm^3) $a = 4.594239$, c = 2.959295 ($R_{wp} = 0.0423$). There is a small peak at about 31.6° (2θ) that remains unidentified. It does not originate from the determined phases present or from $ZnTiO_3$ nor $Zn_2Ti_3O_8$. It could possibly be the high pressure polymorph of TiO_2, peak (1 1 1) [21], or the (1 0 0) peak of ZnO that is more probable [22]. The value of the lattice parameter determined for Zn_2TiO_4 is similar to the value obtained by Kim et al. ($a = 8.4558$) for the 1ZnO·1TiO_2 nominal composition that after sintering at 1150 °C resulted in the presence of zinc orthotitanate and rutile phases [1].

The change of sample density with temperature for samples sintered to 1200 °C is also shown in Fig. 2 where one can see that the density increases until the temperature of about 955 °C when the sample density slightly decreases to about 970 °C after which it again increases linearly. The average final sample density was determined as 93%. Taking into account the phase diagram for the ZnO–TiO_2 system and the phase transitions in this system described with Eq. (1) complete transformation of $ZnTiO_3$ into Zn_2TiO_4 and r-TiO_2 is expected at temperatures above 950 °C and it is accompanied by a slight density decrease due to the difference in molar volume between the low and high temperature phases. The temperature up to which the previously determined MSC curve (with activation energy of 313 kJ/mol) can be applied is 900 °C (Fig. 3) as decomposition of $ZnTiO_3$ into Zn_2TiO_4 and r-TiO_2 occurs in the temperature interval between 900 and 950 °C. Above 900 °C we were not able to define a MSC curve, we attempted to do so in the temperature interval 1000–1200 °C when sintering of the Zn_2TiO_4 and r-TiO_2 mixture takes place, but obviously in this temperature interval two or more sintering mechanisms operate simultaneously. Also, one cannot exclude grain growth during the sintering process. The phase transition of $ZnTiO_3$ into

Zn_2TiO_4 is characterized by nucleation and grain growth [23]. First at temperatures in the vicinity of the true thermodynamic transition temperature while heating and before the new phases appear positions of all atoms correspond to the initial phase. Formation of the new phase is the consequence of fluctuations bringing atoms to new positions. Above a critical volume they form ''nuclei'' of the product phase. The nuclei are formed at a certain rate and they are followed by propagation of the new phase at a faster rate.

4. Conclusion

Sintering of nanosized $ZnTiO_3$ powder to 900 °C results in samples that have a certain amount of porosity (on average 13.8%), but the shrinkage (densification) rate is quite high taking into account the porosity of the starting samples. Also at this temperature sintered samples contain besides $ZnTiO_3$, Zn_2TiO_4 and r-TiO_2 and traces of $Zn_2Ti_3O_8$, but a unique MSC could be defined for the sintering process regardless of the heating rate with a sintering process activation energy of 313 kJ/mol. Sintering of nanosized $ZnTiO_3$ powder to 1200 °C results in samples in which a complete transformation of the starting $ZnTiO_3$ into Zn_2TiO_4 and r-TiO_2 has occurred.

Acknowledgements

The authors would like to express their gratitude to Professor Mao-Hua Teng for enabling use of his MSC computer program. The Ministry for Science of the Republic of Serbia financed this work through project 142011G.

References

[1] H.T. Kim, J.D. Byun, Y. Kim, Microstructure and microwave dielectric properties of modified zinc titanates (II), Mater. Res. Bull. 33 (1998) 975–986.
[2] S.K. Manik, S.K. Pradhan, Preparation of nanocrystalline microwave dielectric Zn_2TiO_4 and $ZnTiO_3$ mixture and X-ray microstructure characterization by Rietveld method, Physica E 33 (2006) 69–76.
[3] Y.-S. Chang, Y.-H. Chang, I.-G. Chen, G.-J. Chen, Y.-L. Chai, T.-H. Fang, S. Wu, Synthesis, formation and characterization of $ZnTiO_3$ ceramics, Ceram. Int. 30 (2004) 2183–2189.
[4] Y.L. Chai, Y.S. Chang, G.J. Chen, Y.J. Hsiao, The effects of heat treatment on the structure evolution and crystallinity of $ZnTiO_3$ nanocrystals prepared by Pechini process, Mater. Res. Bull. 43 (2008) 1066–1073.
[5] X. Liu, M. Zhao, F. Gao, L. Zhao, C. Tian, Effects of WO_3 addition on the phase structure and transition of zinc titanate ceramics, J. Alloys Compd. 450 (2008) 440–445.
[6] O. Yamaguchi, M. Morimi, H. Kawabata, K. Shimizu, Formation and transformation of $ZnTiO_3$, J. Am. Ceram. Soc. 70 (1987) C97–C98.
[7] H.T. Kim, Y. Kim, M. Valant, D. Suvorov, Titanium incorporation in Zn_2TiO_4 spinel ceramics, J. Am. Ceram. Soc. 84 (2001) 1081–1086.
[8] U. Steinike, B. Wallis, Formation and structure of Ti-Zn-oxides, Cryst. Res. Technol. 32 (1997) 187–193.
[9] J. Yang, J.H. Swisher, The phase stability of $Zn_2Ti_3O_8$, Mater. Char. 37 (1996) 153–159.
[10] D. Lance, F. Valdivieso, P. Goueriot, Correlation between densification rate and microstructural evolution for pure alpha alumina, J. Eur. Ceram. Soc. 24 (2004) 2749–2761.
[11] M.-H. Teng, Y.-C. Lai, Y.-T. Chen, A computer program of master sintering curve to accurately predict sintering results, Westr. Pac. Earth Sci. 2 (2002) 171–180.
[12] H. Su, D.L. Johnson, Master sintering curve: a practical approach to sintering, J. Am. Ceram. Soc. 79 (1996) 3211–3217.
[13] D.C. Blaine, S. Park, R.M. German, Master sintering curve for a two-phase material, Sintering'05, in: 4th International Conference on Science, Technology and Application of Sintering, 2005 (August–September), 264–267.
[14] A. C. Larson, R. B. Von Dreele, General Structure Analysis System (GSAS), Los Alamos National Laboratory Report LAUR 86-748.(2004).
[15] B.H. Toby, EXPGUI, a graphical user interface for GSAS, J. Appl. Cryst. 34 (2001) 210–213.
[16] S.F. Bartram, A. Slepetys, Compound formation and crystal structure in the system ZnO–TiO_2, J. Am. Ceram. Soc. 44 (1961) 493–499.
[17] B.A. Wechsler, C.T. Pruwitt, Crystal structure of ilmenite ($FeTiO_3$) at high temperature and high pressure, Am. Mineral. 69 (1984) 176–185.
[18] R.L. Millard, R.C. Peterson, B.K. Hunter, Study of the cubic to tetragonal transition in Mg_2TiO_4 and Zn_2TiO_4 spinels by ^{17}O MAS NMR and Rietveld refinement of X-ray diffraction data, Am. Mineral. 80 (1995) 885–896.
[19] E.F. Meagher, G.A. Lager, Polyhedral thermal expansion in the TiO_2 polymorphs; refinement of the crystal structures of rutile and brookite at high temperature, Can. Mineral. 17 (1979) 77–85.
[20] A. S. Wills, VaList, program available from www.ccp14.ac.uk.
[21] I.E. Grey, C. Lee, I.C. Madsen, G. Braunhausen, TiO_2–II. Ambient pressure and structure refinement, Mater. Res. Bull. 23 (1988) 743–753.
[22] S.C. Abrahams, J.L. Berstein, Remeasurement of the structure of hexagonal ZnO, Acta Cryst. B25 (1969) 1233–1236.
[23] C.N.R. Rao, K.J. Rao, Phase transitions in solids, McGraw Hill Inc, 1978